Catalytic growth of clusters of wurtzite ZnS nanorods through co-deposition of ZnS and Zn on Au film

Changqing Jin,[a] Yingchun Cheng,[a] Xin Zhang,[a] Wei Zhong,*[a] Yu Deng,[a] Chaktong Au,[b] Xinglong Wu[a] and Youwei Du[a]

Clusters of ZnS nanorods have been fabricated by co-deposition of ZnS and Zn on a gold film at 530 °C. The as-obtained product is comprised of uniform ZnS nanorods (about 200 nm in diameter and 1–2 μ in length) with preferred [001] orientation, showing a polar top/bottom surface. The nanomaterials show strong green emission centered at 520 nm at room temperature. The structures and morphologies of the clusters were studied by means of X-ray diffraction, field emission scanning electron microscopy, and high-resolution transmission electron microscopy, and a mechanism for the growth of ZnS nanorods has been suggested.

Semiconductor materials of multifarious nanostructures have been successfully synthesized in the past decade. Some of these materials exhibit novel electronic[1,2] and optical[3] properties as well as quantum-confinement effect.[2,4] Semiconductors of one-dimensional (1D) nanostructures such as nanorods, nanowires and nanotubes, tunable in size, morphology, crystallographic orientation as well as in surface-to-volume ratio are of particular interest in nanotechnology.[5,6] Zinc sulfide (ZnS) belongs to the II–VI semiconductor family and has a room-temperature band gap of 3.7 eV. The material is important in photonics because it is high in refraction index and shows high transmittance in the visible region. Furthermore, ZnS is known to show superconductivity, ferroelectricity, magnetism, and piezoelectricity properties, and has been studied for chemical sensing.[7]

Recently, electrochemical deposition[8] and vapour–liquid–solid (VLS) processes[9] have been adopted to grow ZnS of 1D nanostructures. Much research has been focused on the fabrication of 1D ZnS nanostructures to explore their optical properties,[3,10,16] such as field-emission.[20] For technical applications, 1D nanomaterials are fabricated with particular anisotropic properties such as conductivity and band structure. Semiconductor nanomaterials are generated with aligned and ordered orientation, and arrays of 1D nanostructures with special and preferential orientation are considered as potential building blocks for electronic and optoelectronic nanodevices. For example, Jiang et al. found that cathodoluminescence (CL) is sensitive to the orientation of 1D nanostructures, and prepared cross arrays of ZnS nanowires that can function as Fabry-Perot cavities.[11] Following a vapor transport and condensation process, Huang et al. prepared arrays of ZnO nanowires ([001] oriented) on sapphire

[a]Nanjing National Laboratory of Microstructures and Department of Physics, Nanjing University, Nanjing, 210093, People's Republic of China; Fax: +86-25-83595535; Tel: +86-25-83621200
[b]Chemistry Department, Hong Kong Baptist University, Hong Kong, People's Republic of China

substrates.[12] On the other hand, crystal bundles of ZnS nanowires of ordered orientation were prepared by Moore et al. on a thin CdSe film that was fabricated on a Si (111) substrate.[13]

Herein, we report the synthesis of hierarchically assembled ZnS clusters array comprised of wurtzite ZnS nanorods (in high yield) via thermal evaporation. The preparation process has not been reported before. A quartz tube with id 48 mm and length of 800 mm was installed in a tube furnace. Then a ceramic boat loaded with a mixture of zinc sulfide and zinc (ZnS : Zn molar ratio = 1 : 10) powder was placed in the center of the furnace. A piece of Si(111) substrate with the exposed face coated with Au (30 nm thick) was placed in a ceramic boat located downstream (approximately 8 cm from the center of the source). After evacuation to a base pressure of ca. 10^{-3} Pa by means of pumping, the system was purged with high-purity Ar (used as carrier gas as well) at a flow rate of 20 sccm (standard cubic centimeters per minute). The ZnS and Zn mixture was heated to 750 °C in a span of 1.5 h. Then the mixture was kept at 750 °C for 1 h while the temperature of the Si(111) substrate was maintained at about 530 °C. After the deposition of materials on the substrate, the whole system was cooled to room temperature (RT) and the Ar supply was disconnected.

We found that the yield of product is high, and the generation of the clusters highly reproducible. The crystal structure of the product was determined by X-ray diffraction (XRD) (D/Max-RA, Rigaku, Japan, Cu Kα). As shown in Fig. 1a, the diffraction peaks can be indexed to the wurtzite phase, indicating the formation of ZnS crystallites. The small signals of Au are likely to be due to gold aggregates. We cannot detect any XRD signal of metallic zinc. It is possible that at 530 °C and under a pressure of 10^{-3} Pa, there was rapid vaporization of metallic zinc. We found that the Raman spectrum (200–800 cm^{-1}) collected under N_2 at 80 K over the sample (Fig. 1b) is similar to that of wurtzite-phase ZnS nanowires recorded at room temperature.[14] The SO (341 cm^{-1}) mode is the unique feature of wurtzite-phase ZnS nanostructures, and is absent in the case of cubic-phase ZnS nanostructures. The peak located at 278 cm^{-1} is the A_1 mode and the peak at 353 cm^{-1} is the LO mode of A_1 and E_1 symmetry. The results confirm the formation of wurtzite ZnS phase, in consistence with the XRD results.

Field emission scanning electron microscopy (FE-SEM) and energy dispersion spectroscopy (EDS) were employed to find out the morphology and nature of the product. Fig. 2a and b show the presence of nanorod clusters. According to Fig. 2c–f, the length of the rods is about 1 μ, and the width about 200 nm. Most of the ZnS rods show uniform morphology. Fig. 2e shows that the top ends of the nanorods are uneven, and some small nanorods assemble to form a bigger nanorod. Fig. 2f shows the top of a nanorod is not smooth.
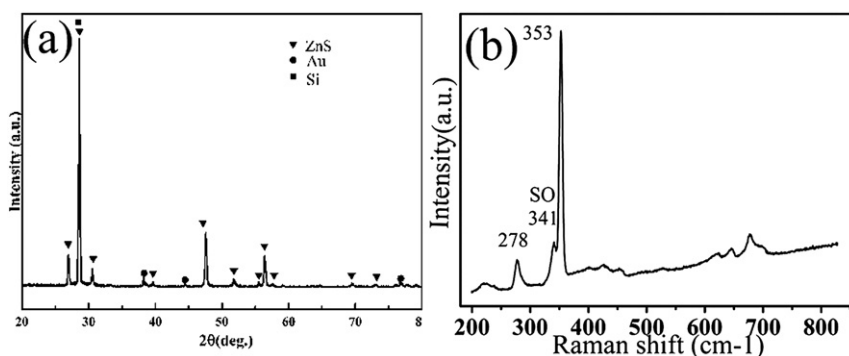
Fig. 1 (a) XRD patterns of ZnS nanorods; (b) Raman spectrum of product acquired at 80 K.
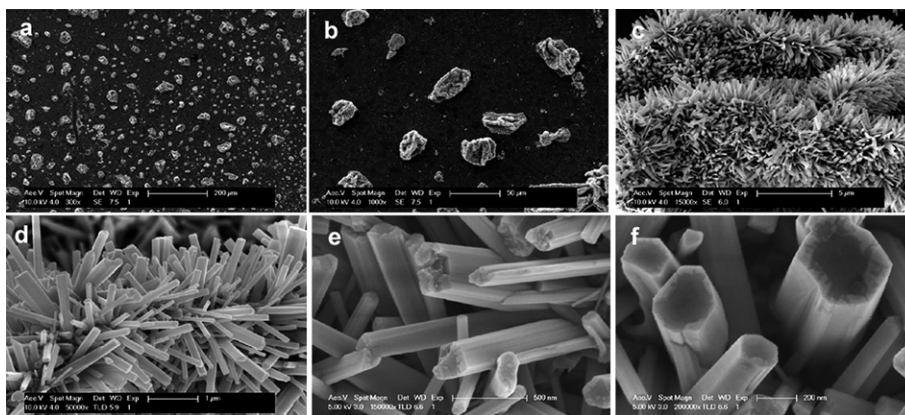

Fig. 2 (a) and (b): FE-SEM images of nanorod clusters in low magnifications, (c) and (d): FE-SEM images of arrays of ZnS nanorods, and (e) and (f): images of the tops of nanorods in high magnifications.
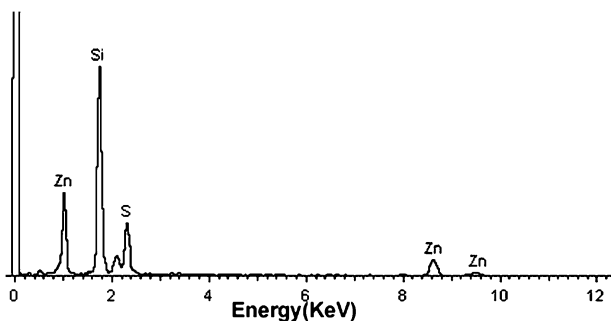

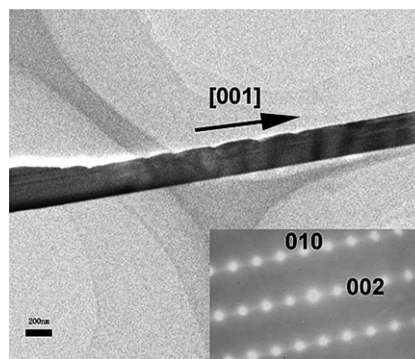**Fig. 3** EDS spectrum of ZnS nanorods.

Fig. 4 TEM and SAED images of a piece of ZnS nanorod.

Fig. 3 shows the atomic contents of Zn and S are almost the same. Shown in Fig. 4 is the TEM image of a single piece of ZnS nanorod. The selected-area electron diffraction (SAED) pattern (inset of Fig. 4) denotes single crystallinity, and can be indexed to reflections along the [100] zone axis of single crystals with hexagonal structure of lattice parameters $a = 3.83$ Å and $c = 6.26$ Å. It is apparent that the [001] direction is preferred in the growth of the nanorods. The corresponding HRTEM image (Fig. 5) shows a lattice space of 0.63 nm, matching that of the (001) planes of wurtzite ZnS. The inset of Fig. 5 shows an atomic model depicting that the top/bottom surfaces are terminated either with Zn or S and are polar in nature. According to the XRD, FE-SEM, TEM and EDS results, it is clear that the clusters are comprised of single-crystalline wurtzite ZnS nanorods.

The photoluminescence properties of the array of ZnS nanorod clusters were investigated at RT using He–Cd laser line at 325 nm as excitation source (Fig. 6a). The spectrum shows a strong green emission (520 nm), and there is no detection of band-gap emission. Samples of nanocrystalline ZnS doped with different levels of Cu^{2+}, Mn^{2+} or rare earth ions are known to show visible-light emissions.[14,15] In a PL study of ZnS nanostructure produced on a gold film, Gong *et al.* detected green emission.[16] Nevertheless, some researchers suggested that the luminescence peak at about 520 nm is due to the recombination of electrons and holes, the former from the energy level of sulfur vacancies (neutral donor) and the latter from the energy level of zinc
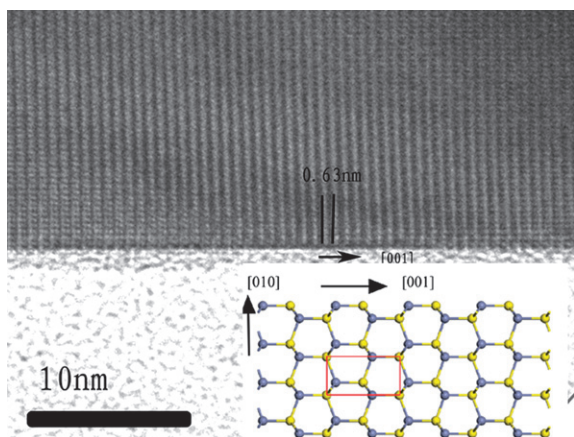
Fig. 5 HRTEM image of a single piece of ZnS nanorod, and the corresponding atomic model that shows ZnS nanorods with polar top/bottom surface.
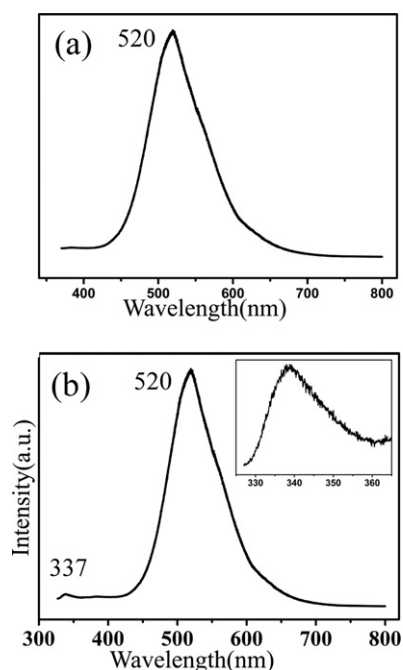

Fig. 7 SEM and TEM images of ZnS nanowires fabricated without zinc at the evaporation source. (a) Low-magnification SEM image of as-prepared ZnS nanowires array on Au-coated Si substrate; (b) high-magnification SEM image, showing the straight and blend nanowires; (c) TEM image of a single piece of ZnS nanowire, (d) high-magnification TEM image of a single piece of ZnS nanowire with a nanoparticle located at the top.

Fig. 6 (a) PL spectrum of product acquired at RT; (b) CL spectrum of product acquired at RT.

Fig. 8 Growth process of nanowires.

vacancies (neutral acceptor) within the band gap (D^0A^0 recombination).[17] We believe that the green emission of Fig. 6a is due to vacancies rather than to Au impurities in ZnS. The EDS results (not shown) collected using the EDX facility of the TEM instrument show no presence of Au in the body of the ZnS nanorods. To find out the origin of luminescence, CL investigation using a tunable light source of shorter wavelength and higher spatial resolution was carried out. The CL spectrum (Fig. 6b) shows weak bandgap emission and stronger green emission centered at about 337 and 520 nm, respectively. The amplificatory image (Fig. 6b, inset) reveals that the weak bandgap emission is especially narrow, showing fwhm (full width at half maximum) of 15 nm. Similar CL spectra are collected at different locations of the sample, reflecting the uniformity of the array.
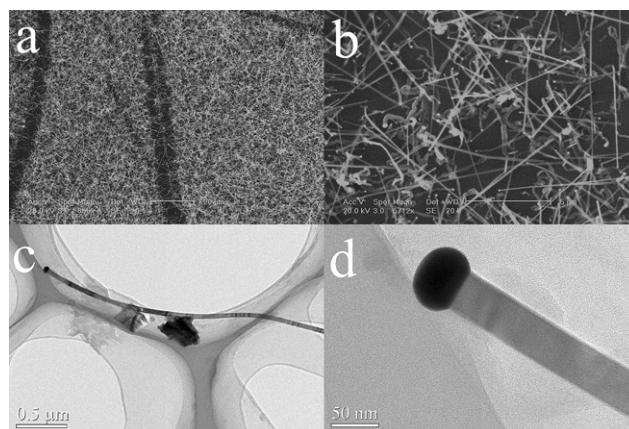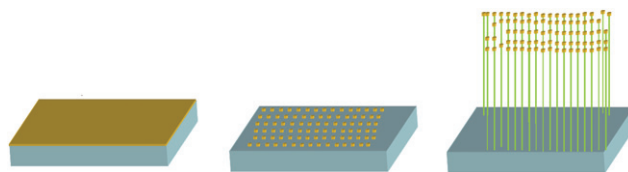
To find out the role of Zn in the fabrication of ZnS nanorods, we performed a control experiment in which only ZnS (rather than a mixture ZnS and Zn) was at the evaporation source. Shown in Fig. 7 are the SEM and TEM images of the as-obtained sample, one can see that ZnS nanowires (tens of microns in length and about 60 nm in diameter) rather than ZnS nanorods are produced. The low-magnification SEM image (Fig. 7a) reveals that the nanowires are grown from separated nucleation sites that seem to be connected. The high-magnification SEM image (Fig. 7b) shows that the nanowires with top nanoparticles are uniform in diameter; blend and straight nanowires can all be found. Fig. 7c is the TEM image of a single piece of nanowire with a top nanoparticle. The high-magnification TEM image of a single piece of nanowire (Fig. 7d) reveals clearly the presence of a nanoparticle at the top of the nanowire, a phenomenon typical of VLS growth.[18,19] We hence deduce that the nanoparticle is made up of gold, and the growth of ZnS nanowires follows a VLS mechanism. First ZnS is evaporated and then diffuses and dissolves into Au liquid droplets. Upon supersaturation of ZnS in liquid Au, there is the precipitation of ZnS at the Au/Si interface. With continuous precipitation and growth of ZnS crystal, the Au liquid droplet becomes separated from the Si substrate, and there is the formation of ZnS nanowires with diameter restricted by the size of the gold droplets (Fig. 8).

Shown in Fig. 9 are the suggested steps for the formation of ZnS nanorods. With increase of substrate temperature, the Au layer becomes liquid droplets (tens of nanometers in diameter) and there is
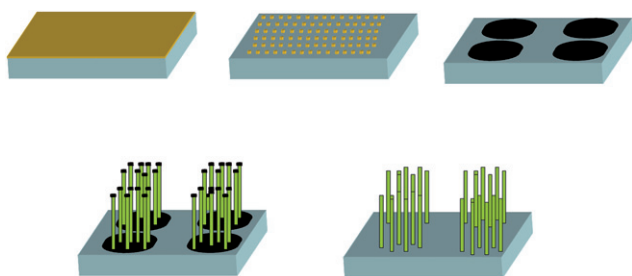
Fig. 9 Growth process of nanorods.

the diffusion and dissolution of Zn into liquid gold. Gradually, the droplets enlarge into Zn/Au patches (micrometers in diameter) which are enriched with Zn. When the Zn/Au phase is supersaturated with ZnS, there is precipitation and crystal growth of ZnS. We suggest that nucleation of ZnS occurs at the Au/Si interface. (No ZnS nanorods and ZnS nanowires can be formed on a Si(111) substrate without the presence of Au.) At the beginning, with the continuous supply of ZnS in the Zn/Au phase, there is continuous growth of ZnS crystals. However, with the evaporation of Zn (at 530 °C and under 10^{-3} Pa), the growth is terminated. That is the reason why ZnS nanorods rather than ZnS nanowires are formed in the case when "Zn + ZnS" is used as evaporation source. As a result, the top of the nanorods is different from that of nanowires; that of the former (Fig. 2e and f) is a bare and rough end while that of the latter is attached with a gold nanoparticle (Fig. 8). It is known that using Zn as a seed is beneficial for the growth of nanorods.[20] It is possible that Zn not only acts as a seed but also as a catalyst when it exists as a liquid droplet on the top of ZnS nanorods during the growth of ZnS crystals.

In summary, clusters of wurtzite ZnS nanorods were fabricated by means of ZnS and Zn co-deposition on a gold film at 530 °C. When only ZnS is at the evaporation source, ZnS nanowires rather than ZnS nanorods are generated. We deduce that the VLS mechanism can be applied to illustrate the growth of ZnS nanorods. The nanorods are about 200 nm in diameter, and 1–2 μ in length, showing aspect ratios of 5–10. The nanorods are single-crystalline with preferential [001] growth direction. We detected strong green emission at 520 nm over the arrays, and believe that the materials are potentially useful in the designs of semiconducting and optical nanodevices.

Notes and references

1 B. Z. Tian, X. L. Zheng, T. J. Kempa, Y. Fang, N. F. Yu, G. H. Yu, J. L. Huang and C. M. Lieber, *Nature*, 2007, **449**, 885.
2 X. S. Fang, Y. Bando, G. Z. Shen, C. H. Ye, U. K. Gautam, M. F. J. Pedro, Costa, C. Zhi, C. C. Tang and D. Golberg, *Adv. Mater.*, 2007, **19**, 2593.
3 Q. H. Xiong, G. Chen, J. D. Acord, X. Liu, J. J. Zengel, H. R. Gutierrez, J. M. Redwing, L. C. Lew Yan Voon, B. Lassen and P. C. Eklund, *Nano Lett.*, 2004, **4**, 1663.
4 A. B. Sharma, S. K. Sharma, M. Sharma, R. K. Pandey and D. S. Reddy, *Spectrosc. Acta, Part A*, 2009, **72**, 285.
5 (*a*) Y. D. Li, H. W. Liao, Y. Ding, Y. T. Qian, L. Yang and G. E. Zhou, *Chem. Mater.*, 2001, **10**, 2301; (*b*) X. F. Duan, C. M. Niu, V. Sahi, J. Chen, J. W. Parce, S. Empedocles and J. L. Goldman, *Nature*, 2003, **425**, 274; (*c*) J. Q. Hu, Y. Bando, J. H. Zhan and D. Golberg, *Angew. Chem., Int. Ed.*, 2004, **43**, 4606.
6 (*a*) A. M. Morales and C. M. Lieber, *Science*, 1998, **279**, 208; (*b*) Z. W. Pan, Z. R. Dai and Z. L. Wang, *Science*, 2001, **291**, 1947; (*c*) Y. C. Zhu, Y. S. Bando and D. F. Xue, *Appl. Phys. Lett.*, 2003, **82**, 1769.
7 Y. Huang and C. M. Lieber, *Pure Appl. Chem.*, 2004, **76**, 2051; C. Borchers1, D. Stichtenoth, S. Miiller, D. Schwen and C. Ronning, *Nanotechnology*, 2006, **17**, 1067.
8 X. J. Xu, G. T. Fei, W. H. Yu, X. W. Wang, L. Chen and L. D. Zhang, *Nanotechnology*, 2006, **17**, 426.
9 Y. Jing, X. M. Meng, J. Liu, Z. R. Hong, C. S. Lee and S. T. Lee, *Adv. Mater.*, 2003, **15**, 1195.
10 X. S. Fang, C. H. Ye, L. D. Zhang, Y. H. Wang and Y. C. Wu, *Adv. Funct. Mater.*, 2005, **15**, 63; D. Moore, Y. Ding and Z. L. Wang, *Angew. Chem., Int. Ed.*, 2006, **45**, 5150.
11 Y. Jing, W. J. Zhang, J. S. Jie, X. M. Meng, J. A. Zapien and S. T. Lee, *Adv. Mater.*, 2006, **18**, 1527.
12 M. H. Huang, S. Mao, H. Feick, H. Q. Yan, Y. Y. Wu, H. Kind, E. Weber, R. Russo and P. D. Yang, *Science*, 2001, **292**, 1897.
13 D. F. Moore, Y. Ding and Z. L. Wang, *J. Am. Chem. Soc.*, 2004, **126**, 14372.
14 Q. H. Xiong, J. G. Wang, O. Reese, L. C. Lew Yan Voon and P. C. Eklund, *Nano Lett.*, 2004, **4**, 1991.
15 (*a*) C. H. Liang, Y. Shimizu, T. Sasaki, H. Umehara and N. Koshizaki, *J. Phys. Chem. B*, 2004, **108**, 9728; (*b*) P. Yang, M. K. Lu, D. Xu, D. L. Yuan and G. J. Zhou, *Chem. Phys. Lett.*, 2001, **336**, 76.
16 J. F. Gong, S. G. Yang, J. H. Duan, R. Zhang and Y. W. Du, *Chem. Commun.*, 2005, 351.
17 H. Y. Lu, S. Y. Chu and S. S. Tan, *J. Cryst. Growth*, 2004, **269**, 385; V. Dimitrova and J. Tate, *Thin Solid Films*, 2000, **365**, 134.
18 Y. F. Hao, G. W. Meng, Z. L. Wang, C. H. Ye and L. Zhang, *Nano Lett.*, 2006, **6**, 1650.
19 R. S. Wagner and W. C. Ellis, *Appl. Phys. Lett.*, 1964, **4**, 89.
20 W. Yu, P. F. Fang and S. j. Wang, *Appl. Surf. Sci.*, 2009, **255**, 5709; X. S. Fang, Y. Bando, C. H. Ye and D. Golberg, *Chem. Commun.*, 2007, 3048.